Cellulose (2019) 26:4767–4786
https://doi.org/10.1007/s10570-019-02400-5

ORIGINAL RESEARCH

Effect of refining and homogenization on nanocellulose fiber development, sheet strength and energy consumption

Shaun Ang · Victoria Haritos · Warren Batchelor

Received: 20 November 2018 / Accepted: 28 March 2019 / Published online: 5 April 2019

Abstract Nanocellulose has great potential for end use in the pulp and paper industry, but its mechanical production process is often extremely energy intensive. Although various pre-treatment methods have been introduced to significantly lower the energy consumption of nanocellulose production, there still remains a great challenge to match the cost to mechanical strength performance of nanocellulose. This research investigates the relationship between energy consumption with numerous refining and homogenization cycles towards the production of high aspect ratio and low diameter nanocellulose, and whether this is necessary to achieve high strength sheets. Never-dried Bleached Eucalyptus Kraft pulp was mechanically treated with a PFI mill refiner and homogenizer. The actual homogenization energy measured on a lab scale was significantly higher than that predicted only from the simplified pressure drop equation which is inaccurately independent of homogenizer design and size. We measured two aspects of fiber quality believed to be related to sheet mechanical strength: the fiber diameter, which is inversely proportional to the surface area available for bonding, and the fiber aspect ratio, which is believed to control the efficiency of stress transfer within a network. Both refining and homogenization reduced the fiber diameter and increased the aspect ratio, but homogenization was more effective at both. There was surprisingly little correlation between the measures of fiber quality and mechanical sheet strength. All PFI mill refined samples had a tensile index of around 100 Nm/g, while additional treatment with homogenization increased this only by approximately 20%. This was despite the most heavily treated fibers (50,000 PFI revolutions and 3 homogenization passes at 1000 bar) having a median diameter of 12 nm and aspect ratio of 229 compared to the least treated fibers (10,000 PFI revolutions) with a median diameter of 31 nm and aspect ratio of 102. The most heavily treated fibers required 39,000 kWh/t of energy, a tenfold increase over the least heavily treated fibers. The results confirmed that there was small benefit, in terms of mechanical strength, of using very large amounts of energy to produce very low diameter, high aspect ratio nanocellulose fibers.

Electronic supplementary material The online version of this article (https://doi.org/10.1007/s10570-019-02400-5) contains supplementary material, which is available to authorized users.

S. Ang · V. Haritos · W. Batchelor (✉)
Bioresource Processing Research Institute of Australia, Department of Chemical Engineering, Monash University, Melbourne, VIC 3800, Australia
e-mail: warren.batchelor@monash.edu

Graphical abstract

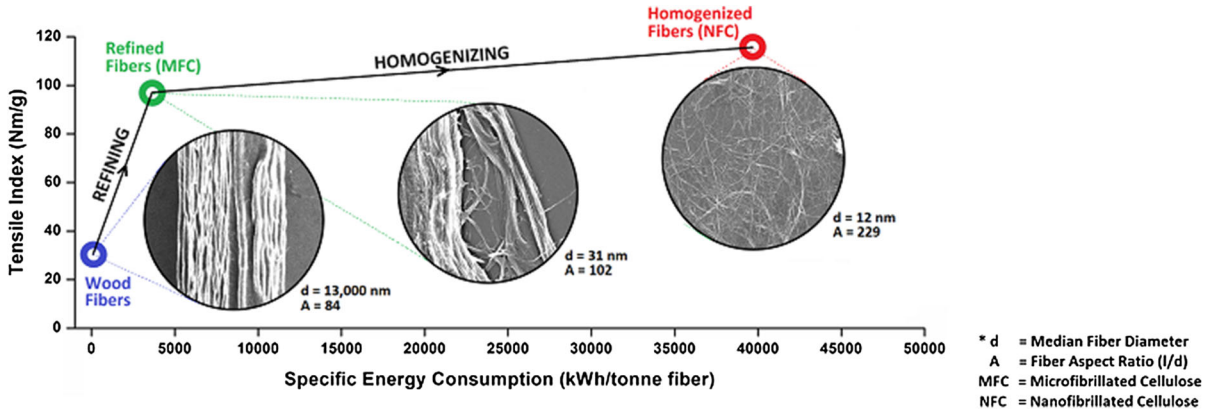

Keywords Nanocellulose · Energy consumption · Strength · Aspect ratio · SEM

Introduction

The 3 order of magnitude reduction in fiber dimensions that occurs when cellulose fibers are broken down into elementary microfibrils allows for the production of a unique class of cellulose nanomaterials which have high strength, high specific surface area, high elastic modulus, high thermal coefficient, low toxicity, good biodegradability and good barrier properties (Lavoine et al. 2012; Osong et al. 2016; Siró and Plackett 2010).

The many applications of nanocellulose include food packaging (Aulin et al. 2010), reinforcements for nanocomposite fillers (Ramires and Dufresne 2011), anti-microbial films (Andresen and Stenius 2007) and flexible electrodes for lithium ion batteries (El Baradai et al. 2016). The unique rheology and viscoelasticity of cellulose nanomaterials have also been highlighted for various uses such as coatings for paper manufacturing with carboxymethyl cellulose (Dimic-Misic et al. 2013), UV shielding composites made from nanocrystalline cellulose (Chang et al. 2013), cosmetics with cellulose nanofibrils (Nelson et al. 2016), binder formulations (Dimic-Misic et al. 2014), medical drug delivery with cellulose nanocrystals (Lewis et al. 2016) and paper-based applications (Campano et al. 2018; Syverud and Stenius 2009), the last of which is the focus of this research. The term nanocellulose sheet is often used to define a 2D material made from nanocellulose fibers into a handsheet within a laboratory context, or paper, paper sheet and board within an industrial end application context. It has high strength, foldability and optical translucency (Eichhorn et al. 2001). It has great potential to be used for high strength packaging, electronics (Nogi et al. 2009), novel cellulose-based filters and to greatly simplify the roll-to-roll operations of functional coating on paper (Zhang et al. 2012).

The various methods of mechanical and chemical treatments for cellulose nanomaterial production have been reviewed extensively in the literature (Eichhorn et al. 2010; Isogai et al. 2011b; Lavoine et al. 2012; Osong et al. 2016; Siró and Plackett 2010). Mechanical treatments work by subjecting fibers to large shearing forces which fibrillate and liberate elementary microfibrils. This promotes the development of nanocellulose with high aspect ratios which improves entanglement in fiber networks. Common mechanical treatments include: mechanical refiners (Kerekes 2005), homogenizers (Nakagaito and Yano 2005; Raj et al. 2016; Siró et al. 2011), microfluidizers (Ferrer et al. 2012; Siqueira et al. 2009) and grinding equipment (Iwamoto et al. 2005). A PFI mill is a low consistency refiner that works by rapidly applying a high ratio of compressive to shearing force (Kerekes 2005) to fibrillate fibers pressed between two parallel surfaces rotating under a constant load. This results in high internal fibrillation, but has limitations such as low external fibrillation and fiber shortening (Kerekes 2005). Low consistency refining is more common with chemical pulps while thermomechanical pulps are

often produced at a high consistency of about 30 wt% (Kerekes 2015). Refining at high consistency however does have its challenges due to the complex rheology of suspensions and issues of refiner clogging at a high consistency (Kerekes 2015). Low consistency refining does offer some advantages such as easier pulp handling, pumping and potentially lower energy consumption owing to a more uniform distribution of fibers along the length of the bar (Kerekes 2015). With the homogenizer, the fiber is pressed through a very narrow slit between a pressurized valve and valve seat under high pressure (Klemm et al. 2011). This results in hydrodynamic cavitation and very large shearing forces to liberate the elementary microfibrils (Karande et al. 2013).

Nanocellulose can be produced from a wide variety of cellulose sources including hardwoods (Spence et al. 2010), softwoods (Iwamoto et al. 2008), hemp, sugarbeet (Vartiainen et al. 2015), wheat straw and soy hulls (Alemdar and Sain 2008) and food waste, such as carrot pomace (Varanasi et al. 2018). The fiber dimensions in each nanocellulose subclass are well defined in accordance with ISO TC229 standards (Walker 2012). Microfibrillated cellulose (MFC) also known as cellulose microfibrils (CMF), refer to the larger nanocellulose fibers with diameters in the range of 10–100 nm and lengths of more than 1 μm. Nanofibrillated cellulose (NFC) also known as cellulose nanofibrils (CNF), refer to the smaller fibers with diameters in the range of 4–20 nm and lengths of more than 1 μm. Within the confines of this research, MFC refers to the larger nanocellulose fibers produced with heavy refining while NFC refers to the smaller nanocellulose fibers produced by subjecting highly refined fibers to high pressure homogenization. It is worth noting that these naming conventions are not always limited to these select combinations of mechanical treatments, but were used in this research to simplify sample naming.

Many literature sources have noted that increasing the energy consumption with refining and homogenization reduces the fiber diameters of various feedstocks (Karande et al. 2013; Raj et al. 2016; Spence et al. 2011). However, increasing the degree of refining and homogenization passes for NFC production comes at the expense of very high energy consumption (Kumar et al. 2014). In the case of homogenization, prominent examples include mechanical energy consumption upwards of 27,000 kWh/t with sulphite pulp (Ankerfors 2012), 70,000 kWh/t with Kraft pulp (Eriksen et al. 2008) and 10,000 kWh/t per homogenizer pass with radiata pine pulp (Syverud et al. 2011). As such, pre-treatment methods such as TEMPO-mediated oxidation (Isogai et al. 2011a) and mild enzymatic hydrolysis (Henriksson et al. 2007) are commonly performed to reduce the energy consumption. However, criticisms such as the high cost and toxicity of TEMPO (Osong et al. 2016), and difficulty in harvesting the nanocellulose before excessive hydrolysis to soluble sugars with enzymes (Vigneshwaran et al. 2015) have been raised.

Thorough understanding of nanocellulose dimensions through fiber characterization techniques is key to tailor nanocellulose for specific applications such as sheet formation, where the size of filter pores and drainage times depend largely on fiber diameters (Zhang et al. 2012) and for paper strength, where the fiber length is critical as evidenced by the Page equation for wood fiber sheets (Page 1969). This has been the area of much research in recent decades. Microscopic techniques such as scanning electron microscopy (SEM), transmission electron microscopy (TEM) and atomic force microscopy (AFM) coupled with image analysis techniques have been used to measure fiber diameter distribution (Pääkko et al. 2007; Raj et al. 2016). Fiber length however, is often more difficult to measure due to the highly entangled fiber networks and difficulty in identifying the fiber ends with SEM images at high magnifications (Henriksson et al. 2008). Sedimentation experiments have been developed for nanocellulose fibers (Varanasi et al. 2013; Zhang et al. 2012) based on original work done on wood fibers (Martinez et al. 2001). This has been noted to be a simple yet effective tool to obtain the gel point of a fiber suspension and correlate that to the aspect ratio (length/diameter) of the fibers based on empirical Effective Medium theory (EMT) (Celzard et al. 2009).

Strength improvements by using nanocellulose fibers have been well documented in the literature (Klemm et al. 2011; Osong et al. 2016; Taipale et al. 2010). One study noted that tensile index and toughness increases by a factor of 4–5 times for MFC films as compared to wood fiber sheets due to improvements in density (Spence et al. 2010). The addition of even small amounts of MFC to wood fiber sheets will improve the sheet strength (Su et al. 2013). MFC films produced from Kraft pulp also showed significant

improvements in bending strength and Young's modulus (Nakagaito and Yano 2005). While some researchers report the use of upwards of 15–20 passes with a homogenizer (Karande et al. 2013; Spence et al. 2011) to obtain a desired fiber quality, this will consume large amounts of energy.

Again, although it is widely accepted that an increase in mechanical treatment and energy input would result in a decrease in fiber dimensions, the correlation between these nanoscale dimensions and sheet strength is not well understood. One study subjected spruce softwood pulp to refining and up to 50 homogenization passes at 50 MPa (Stelte and Sanadi 2009). AFM measurements revealed that the final cellulose nanofiber product after 50 passes had diameters in the 10–25 nm range with aggregates less than 100 nm in diameter (Stelte and Sanadi 2009). The average fiber diameter was believed to decrease with homogenization passes, but the progressive change with each pass was not tracked (Stelte and Sanadi 2009). The refined sheets produced had an average tensile strength of about 50 MPa which increased to 80 MPa with homogenization but remained approximately constant even after 50 homogenization passes (Stelte and Sanadi 2009). Work done on *Pinus Radiata* using a grinder noted that the nanofibers produced had widths of about 20–50 nm after 5 passes and had relatively constant stress at break values of about 90 MPa up to 9 passes (Iwamoto et al. 2007). Results from cotton fiber NFC production with heavy refining revealed that the average fiber diameter decreased from 25,000 nm to 394 nm after 5 passes and to 242 nm after 30 passes through a disc refiner (Karande et al. 2011). Analysis of sheet mechanical properties showed relatively constant stretch % and breaking lengths even after 10 to 30 passes through the refiner (Karande et al. 2011). A separate study investigated the addition of cellulose nanofibrils produced using multiple homogenization passes to reinforce hydroxypropyl cellulose films (Lee et al. 2009). The fiber diameter was measured between 28 and 100 nm after 10 passes and was believed to be even lower after 20 passes but this was not measured (Lee et al. 2009). The addition of 3 wt% nanofibrils produced after 5 passes increased the tensile strength of the composite hydroxypropyl cellulose film from 18 MPa to about 23 Mpa (Lee et al. 2009). However, this strength value remained relatively unchanged even after the addition of fiber produced using 20 homogenization passes (Lee et al. 2009). From the multiple studies noted above, increasing amounts of mechanical treatment do not always produce increases in strength with many cases noting a plateau in strength.

While there are specific applications where very small nanocellulose fiber dimensions are desirable, as in the case of fine cellulose-based filters (Zhang et al. 2012), a question is often raised on the need for such small fibers for nanocellulose sheet strength at the expense of large mechanical energy costs. A reduction in fiber dimensions increases the fiber surface charge which has been noted to reduce fiber agglomeration and clogging issues with refiners (Dimic-Misic et al. 2018b) and homogenizers (Lindström 2017). However, the presence of progressively smaller fibers would also increase the gelation of the fiber suspension (Dimic-Misic et al. 2018b). This has been linked to drawbacks such as suspension dewatering issues, increased transportation costs and reduced processability (Dimic-Misic et al. 2018b). The introduction of MFC and NFC into the paper furnish allows for the addition of a large amount of cheap pigment due to the high surface area of the fibrils and the inter-fiber hydrogen bonds formed (Rantanen et al. 2015). This also raises the question as to whether very small fibrils at the expense of very high energy consumption are necessary. This cost to performance criteria of nanocellulose must be taken into consideration for economic and sustainable production.

In this paper, we investigated the effect of nanocellulose mechanical treatment on fiber quality and sheet mechanical properties and correlated these results to the mechanical energy consumption. Progressive fiber fibrillation and fiber quality was characterized using SEM images to measure the fiber diameter dimensions and gel point sedimentation to estimate the fiber aspect ratio. The results showed that median fiber diameter decreases and aspect ratio increases significantly with mechanical energy consumption. The nanocellulose fibers were then formed into handsheets and their mechanical properties were measured. Interestingly, the most heavily refined and homogenized sample had only marginal strength improvements over the least heavily refined sample, but required a more than tenfold increase in energy consumption to make. There was surprisingly little correlation between the measures of fiber quality (diameter distribution with SEM image analysis and aspect ratio estimation with

gel point sedimentation) and handsheet sheet strength. Here, we have shown that very strong nanocellulose sheets can be produced from larger diameter nanocellulose fibers with heavy refining using much lower energy.

Experimental

Materials

Never-dried unrefined bleached eucalyptus Kraft (BEK 0K) pulp was supplied from Australian Paper Maryvale. BEK was selected as a starting material due to its abundance and long-standing history as a feedstock for papermaking. BEK hardwood fibers are approximately 10–15 μm in diameter and 1 mm in length. Large scale nanocellulose production with a commodity fiber like BEK would be advantageous due to the availability and familiarity of this as a fiber source.

Methods

Mechanical refining as a pre-treatment

BEK fibers were mechanically pre-treated using a PFI mill at 10 wt% in accordance with TAPPI T248 standards (TAPPI 2001a). The number of PFI mill refiner revolutions were set to one of 10,000 (BEK 10K), 30,000 (BEK 30K) and 50,000 (BEK 50K). After PFI refining, the BEK fibers were collected and disintegrated for 15,000 revolutions at 1.2 wt% with a 3L Mavis Engineering (Model No. 8522) standard disintegrator. Standard mechanical disintegration after PFI refining is consistent with the TAPPI T248 standard of laboratory beating of the pulp. Although the changes in fiber morphology with disintegration were not tracked, disintegration was performed consistently across all 7 fiber samples to form a dilute and uniform suspension. Each sample was divided into two. One part was sent directly for papermaking and the other part was treated with high pressure homogenization (HPH) prior to papermaking. From previous experience, a minimum mechanical pre-treatment of 10,000 revolutions was required to prevent clogging of the homogenizer. A summary of fiber sample naming conventions and treatment types is shown in Table 1. To check the repeatability, two batches of BEK 10K and BEK 10K1P were made.

Production of NFC with high pressure homogenization

The refined pulp was homogenized using a GEA Niro Soavi Homogenizer (PANDAPLUS 2000) at a fixed pressure of 1000 bar at 1 wt%. The BEK 10K and BEK 30K refined fibers were sent for 1 pass through the homogenizer to produce BEK 10K1P and BEK 30K1P, respectively. BEK 50K refined fibers were homogenized for 3 passes to produce BEK 50K3P. BEK 50K3P was chosen as the extreme case for the data set and represents the upper limit of mechanical energy consumption (39,000 kWh/t fiber) beyond which the process becomes economically unattractive. The chosen data set allows for the comparison of noticeably different fiber fibrillation qualities on sheet strength. Homogenizer energy usage is dependent on many factors such as homogenizer design, size, operating pressure and fiber suspension consistency to name a few. A homogenization pressure of 1000 bar and suspension consistency of 1 wt% was selected based on previous experience with this instrument. This results in the production of heavily fibrillated nanocellulose while still preventing clogging.

Specific energy consumption

The mechanical energy consumption with both PFI refining and homogenization was measured using a Hager EC350 Three-Phase kWh-meter. It is worth noting that all experimental energy consumption values measured and expressed as kWh/t fiber in this research refer to kilowatt-hour per oven-dry tonne of fiber. The energy measurements were performed twice for each sample to check for repeatability. The total mechanical energy consumption measured in kWh with each run was then divided by oven dried fiber mass (in the case of the refiner) and by fiber suspension mass and concentration (in the case of the continuous homogenizer) to convert to kWh/t fiber. The specific energy consumption values measured were then compared with the values obtained from the pressure drop equation, $W_c = [(P_2 - P_1) \times 1/\rho]/c$, where W_c is the homogenization work in kWh/t fiber, P_1 is the atmospheric pressure, P_2 is set pressure of the homogenizer at 1000 bars, ρ is the density of the

Table 1 Fiber naming conventions and treatment types

Sample	PFI mill refining revolutions	Homogenization passes at 1000 bar
BEK 0K	0	0
BEK 10K	10,000	0
BEK 30K	30,000	0
BEK 50K	50,000	0
BEK 10K1P	10,000	1
BEK 30K1P	30,000	1
BEK 50K3P	50,000	3

suspension and c is the suspension consistency which converts wet tonne of fiber suspension to dry tonne of fiber (Ankerfors 2012).

Surface charge measurements

The surface charge of BEK 0K, BEK 10K and BEK 50K3P were measured as a useful check to ensure both refining and homogenization were progressively fibrillating the fibers. Zeta potential measurements were performed for these suspensions with a Nanobrook Omni (Brookhaven Instruments) in a cuvette cell at 25 °C. The zeta potential was calculated using the provided software by determining the electrophoretic mobility from an electrophoresis experiment using laser Doppler velocimetry and applying the Smoluchowski equation.

SEM imaging and diameter distribution

For SEM imaging sample preparation, fiber samples were first diluted to 0.001 wt%. A single drop of the suspension was cast on top of a silicon chip and left to air dry. The samples were then coated with iridium before imaging. This process was repeated for all fiber samples. SEM images were then taken using an FEI Magellan 400 XHR FEGSEM fitted with a monochromator at a 3.0 kV spot size and 6.3 pA current.

To obtain a fair and unbiased representation of the fibers in an image, the methodology applied was adapted and improved from that given in (Zhang et al. 2012). For each fiber sample, a SEM image which best represented the fiber sample was first taken at a low magnification of 175 × (400 μm scale bar) to capture the large fibers. This image was then divided into 4 quadrants and a 60,000 × (1 μm scale bar) high magnification image was taken in each quadrant. To avoid bias fiber selection, all observable fibers in each SEM image were counted with Image J processing software by measuring the fiber diameters as image pixels and correlating that to a length scale. Care was taken to ensure each observable fiber was only measured once. More than 16,000 fibers were measured in total, with more than 4000 fibers measured for the most heavily treated sample. From the low magnification images, the larger fiber diameters of all samples were sorted into 2000 nm sized bins. From the high magnification images, the nanocellulose fiber diameters were sorted into 5 nm and 2 nm sized bins. This was done using OriginPro 8 software. The value of the bin centre was used for calculations. The fiber counts were normalized by image area to counts/m^2 which allowed for a fair comparison at different magnifications. It is worth noting, for the high magnification images with unrefined BEK 0K, there was typically 1 intact fiber measured per image. We only analysed images with a fiber which when normalized by the area assumes the same concentration of fibers repeating per m^2 of the image. This does not take into account the blank spaces between the unrefined fibers but was still performed to allow for comparison between unrefined, refined and homogenized fibers at high magnification. As such, trends between fiber samples were only observed for a given magnification and not between magnifications. Detailed SEM images for all fiber samples before and after image analysis can be found in the supplementary information.

Sedimentation and gel point determination

Sedimentation tests were conducted with 250 mL fiber suspensions at concentrations ranging between 0.1 wt% and 0.005 wt% for each sample. Each suspension

was thoroughly mixed using a Kambrook hand stirrer (Model Number KSB7) before being poured into a measuring cylinder. The initial sediment height was measured (h_o). The fiber suspension was then left to settle under gravity, for a minimum of 48 h before the final sediment height was measured (h_s). The initial solids concentration (φ_o) was then plotted against the ratio of final sediment height to initial sediment height (h_s/h_o) to determine the gel point of the suspension (Varanasi et al. 2013). By definition, the gel point is the lowest solids concentration at which the fibers form a continuous network.

For each sample, the data of initial solids concentration (C_o) versus (h_s/h_o) was fitted with a smoothing spline (CSAPS, smoothing parameter of $p = 0.998$) in MATLAB following (Raj et al. 2015). The constant y-intercept value at the origin of the first derivative curve gives the gel point.

Aspect ratio estimation

The gel points obtained via sedimentation were used to estimate the aspect ratio of all wood and nanocellulose fiber samples using EMT theory for an assumed cellulose skeletal density of 1500 kg/m^3 (Varanasi et al. 2013). The equation used was $A = 3.19\ C_c^{-0.58}$ where A is the aspect ratio of the fibers and C_c is the solids concentration of the suspension at the gel point (Varanasi et al. 2013). It should be noted that both the low and high magnification fibers have been assumed to have the same aspect ratio, which is unlikely to be correct, but we have used it estimate the indicative length of both the larger and smaller fibers. This was done by multiplying the estimated aspect ratio with the median fiber diameter for the high and low magnification images, separately.

Handsheet making

Within the context of this research, the terms sheet or nanocellulose sheet are used to define a laboratory scale handsheet formed under these conditions. PFI mill refined and homogenized pulp suspensions were made into standard circular handsheets using an Automatic British Handsheet Maker (handsheet diameter of 0.159 m). All pulp suspensions were diluted to 0.2 wt% and mixed with a hand blender for even fiber dispersion prior to sheet making. 60 gsm sheets were formed using 1.2 oven dried grams of fiber suspension. GE Whatman 541 Hardened Ashless filter paper (22 µm pore size) was used on top of a standard 150-size drainage mesh (104 µm pore size) which minimized fiber losses and ensured near 100% fiber retention. For each fiber sample, 3 circular handsheets were made. After conditioning and thickness measurements, the 3 handsheets were cut with a cutting template to obtain as many 10 cm long strips as possible.

Handsheet conditioning and property measurements

Handsheets were conditioned at 50% relative humidity (RH) and 23 °C for a minimum of 24 h prior to testing in accordance with TAPPI T402 standards (TAPPI 2001b). The sheet thickness was measured as an average of 10 random points for each sheet using an L&W Micrometer. Stress–strain load measurements were performed to fracture using an Instron Model 5566 Universal Testing Machine in accordance with TAPPI T494 standards (TAPPI 2001c).

More than 15 separate 10 cm strips (from 3 handsheets) were evaluated for stress–strain load measurements for each fiber sample. Cumulatively, this allowed for approximately 100 measurements across all 7 fiber samples. ANOVA analysis was performed on the refined (BEK 10K, BEK 30K, BEK 50K) versus the refined and homogenized (BEK 10K1P, BEK 30K1P, BEK 50K3P) samples to determine statistical significance and 95% confidence intervals were calculated. The strips from the tensile tests were then collected and dried at 105 °C in a Thermoline BTC-9090 oven to determine the sheet grammage and density.

Results and discussion

Specific energy consumption

The specific energy consumption values measured are summarised in Table 2. Repetitions for the energy consumption measurements resulted in consistent values of 7200 kWh/t fiber for the cases of BEK 10K to BEK 10K1P, BEK 30K to BEK 30K1P, BEK 50K to BEK 50K1P and BEK 50K1P to BEK 50K2P. In the case of BEK 50K2P to BEK 50K3P, the energy consumption values had slight variations between

Table 2 Specific energy consumption measured for all fiber samples

Sample	Specific energy consumption (kWh/t fiber)
BEK 0K	0
BEK 10K	3542
BEK 30K	10,625
BEK 50K	17,709
BEK 10K1P	10,742
BEK 30K1P	17,825
BEK 50K3P	39,309

7000 and 7400 kWh/t fiber, with 7200 kWh/t fiber being the most commonly occurring measurement and average for this continuous homogenizer. Comparing the energy consumption values, for this homogenizer, a single pass at 1000 bar for a 1 wt% suspension is equivalent to approximately 20,300 revolutions in the PFI mill.

It is worth noting that the specific homogenization energy measured using this power meter was much higher than that predicted from only the pressure drop equation in literature (Ankerfors 2012), as shown in the Methods section. This pressure drop equation is however, inaccurately independent of homogenizer design and size (Raj et al. 2016) and does not take into account the type of pulp such as chemical or mechanical pulp, which is believed to affect the energy consumption. As an example, estimations from the pressure drop would for a 1 wt% consistency suspension at 1000 bars operational pressure result in a value of 2775 kWh/t fiber per pass. Under the same conditions, the actual energy consumption measured with the power meter for this lab scale homogenizer was 7200 kWh/t fiber per pass, which is 159% higher than that predicted from the pressure drop.

Surface charge measurements

The zeta potential values of BEK 0K, BEK 10K and BEK 50K3P were measured to be − 11 mV, − 19 mV and − 31 mV respectively. As shown, the zeta potential values become increasingly negative with more refining and homogenization. These results are consistent with progressive mechanical treatments which increases the fiber surface charge (Dimic-Misic et al. 2018a) indicating that progressive fiber fibrillation is occurring for all samples.

SEM imaging and diameter distribution

SEM images of the starting material of never-dried unrefined bleached eucalyptus Kraft (BEK 0K) fiber are shown in Fig. 1. The SEM images displayed in Figs. 2 and 3 show the changes in BEK fiber morphology with progressive refining and homogenization. The shearing forces applied during mechanical refining initiates the process of fiber fibrillation, with the larger fibers showing signs of fraying. Increasing the degree of mechanical refining and homogenization further aids in the breakdown of the wood fibers to produce and liberate nanocellulose fibers that have significantly smaller dimensions.

It is worth noting that progressive refining and homogenization has been known to shift the rheology of the fiber suspension to be more gel-like in behaviour. This phenomenon has been extensively reviewed in the literature (Hubbe et al. 2017). The progressively large number of fibril contact points entraps water on both the fibril surface as immobilized water and in the interfibril spacing which forms the gel structure (Dimic-Misic et al. 2016). The increased water content could potentially result in wall-slip effects occurring with the refiner and homogenizer which reduces processing efficiency. As far as it was observed with this data set up to 50,000 PFI mill revolutions and 3 homogenization passes at 1000 bar, all samples still showed notable changes in fiber diameter and aspect ratio. Further work might be to investigate the effect of nanofiber size on fiber suspension rheology, to determine the point at which refining would have little to no effect.

With highly homogenized NFC fibers in Figs. 2 and 3, most of the fibers can be seen to exist in the nanometer scale based on the high magnification images. Again, it is worth noting that SEM images for all fibers sets were taken at the same 0.001 wt% fiber concentration. Detailed SEM images for all fiber samples before and after image analysis can be found in the supplementary information. As shown in Fig. 3, BEK 50K3P is the most homogenous of all samples with the smallest median fiber dimensions observable with both the low and high magnification images. Interestingly, increasing the mechanical energy consumption progressively shifts the state of the fiber

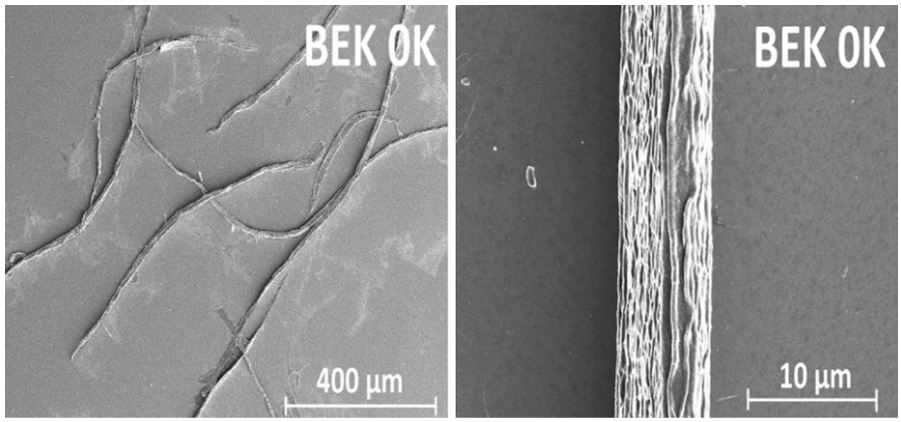

Fig. 1 SEM image of never-dried BEK fibers (BEK 0K) at **a** low magnification and **b** high magnification

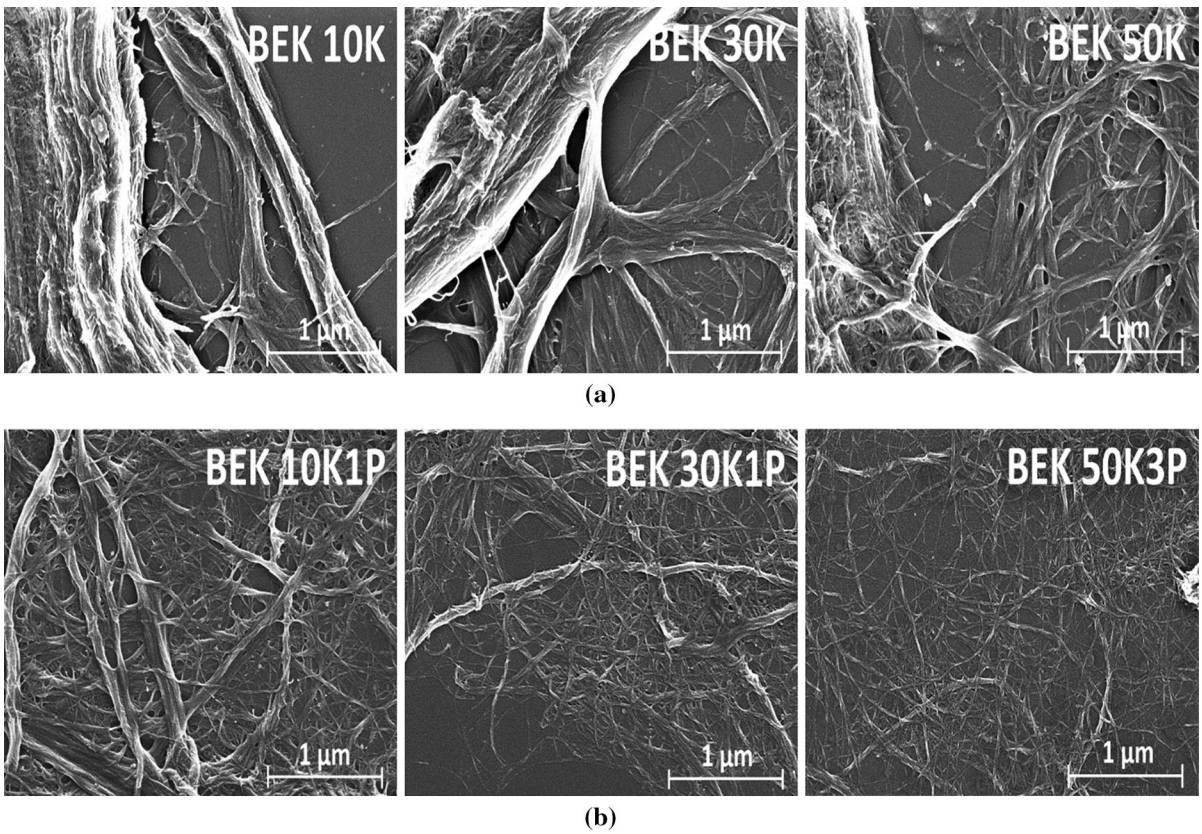

Fig. 2 High magnification SEM images of **a** refined and **b** refined and homogenized fibers. (BEK 50K3P is an abbreviation for bleached eucalyptus kraft nanocellulose fiber which has undergone 50,000 PFI mill refiner revolutions and 3 high pressure homogenization passes at 1000 bar)

suspension from a more heterogeneous mixture with both distinctly large and small fibers, towards a more homogeneous mixture with smaller fiber diameters. This has the potential to be used for applications such as novel nanocellulose filters to ensure uniform filtration and sheet formation spray systems

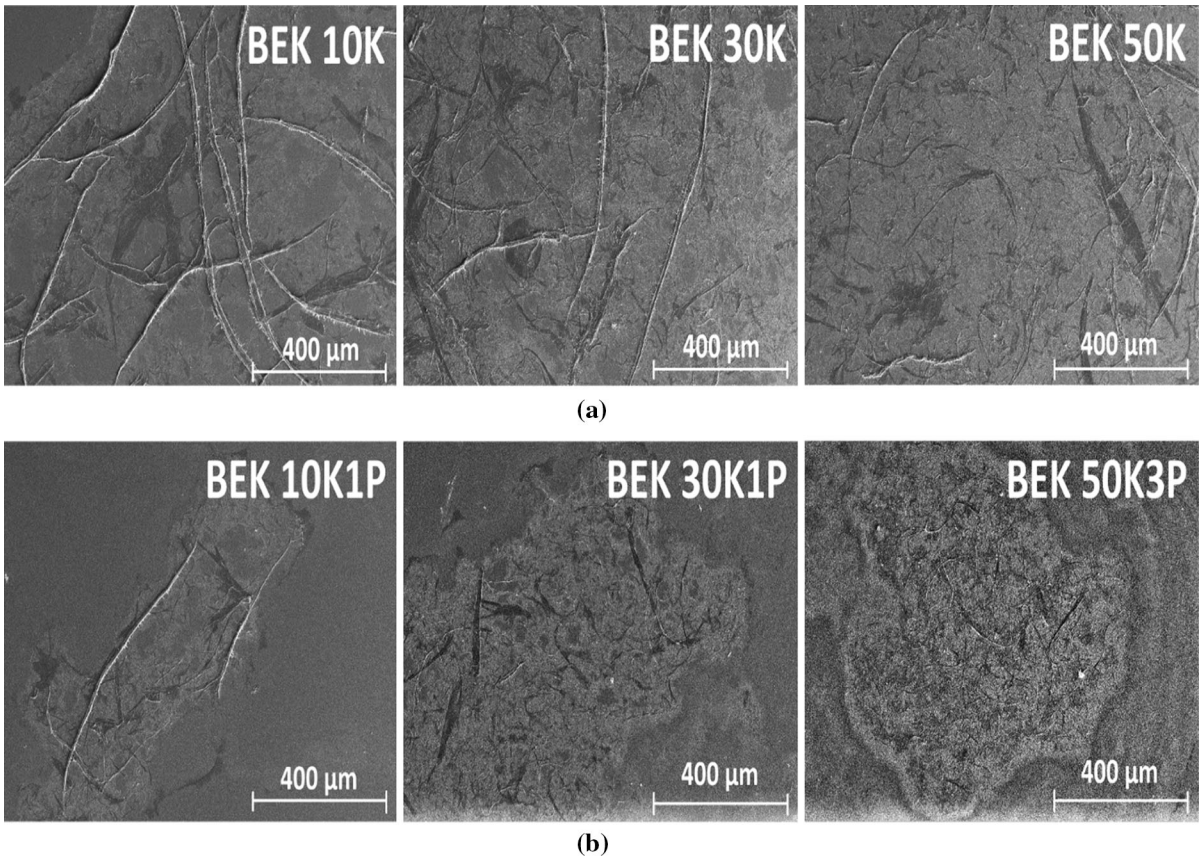

Fig. 3 Low magnification SEM images of **a** refined and **b** refined and homogenized fibers (BEK 50K3P is an abbreviation for bleached eucalyptus kraft nanocellulose fiber which has undergone 50,000 PFI mill refiner revolutions and 3 high pressure homogenization passes at 1000 bar)

(Shanmugam et al. 2018) to prevent nozzle clogging, where the necessity for smaller fiber dimensions is a critical parameter.

Understanding of fiber quality development with mechanical energy is key to tailor nanocellulose fibers with specific diameters and length. The fiber diameter distribution from SEM image analysis is shown in Figs. 4, 5 and 6, for all fiber samples at low magnification, refined MFC fiber samples at high magnification and homogenized NFC fiber samples at high magnification, respectively. Tables 3 and 4 show the minimum, median, maximum, skewness, kurtosis, arithmetic mean, standard deviation, standard error of mean and peak frequency bin center diameter of fiber diameters for the smaller nanocellulose fibers at high magnification, and the larger wood fibers at low magnification, respectively.

From Tables 3 and 4, discrete statistical analysis of all fiber diameter measurements revealed that most refined MFC and homogenized NFC fiber diameter data sets had large positive skewness values. This indicates a long right-tail-end distribution with very few larger diameter fibers in comparison to the number of the smaller nanocellulose fibers. Further analysis of the high magnification images revealed that all data sets had very large positive kurtosis values. This indicates that the fiber distribution is leptokurtic, exhibiting a sharp peak. This is also consistent with a large proportion of the fibers having a small diameter, as evidenced by the heterogeneous nature of the samples from SEM imaging. Due to this, the measures of standard deviation, standard error of mean and arithmetic mean are not suitable to describe this data set which exhibits an asymmetrical distribution. This is supported by the difference in arithmetic mean and median values shown in Tables 3 and 4 indicating a notable deviation from normal. As such, the median was instead chosen as a better representation of central

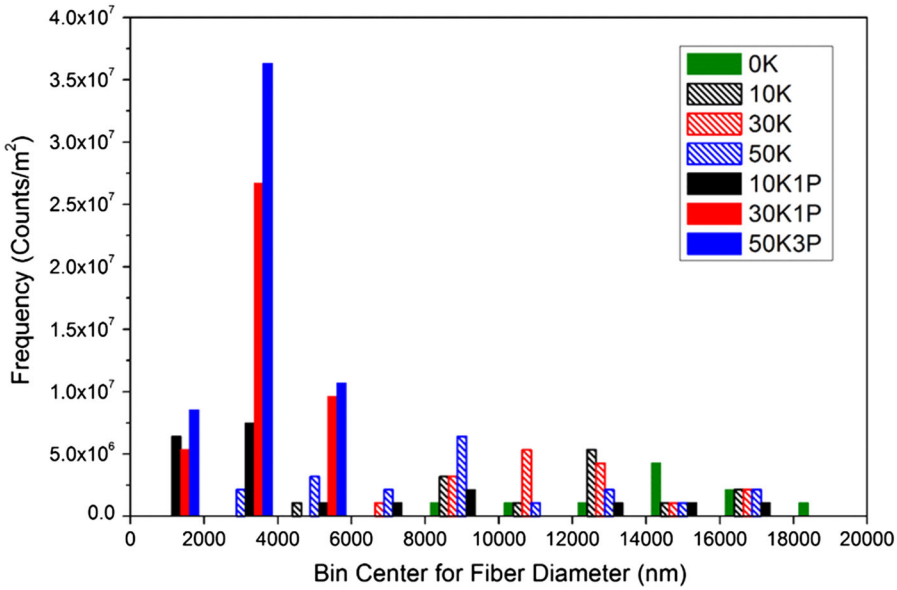

Fig. 4 Diameter distribution of unrefined, refined and homogenized BEK fiber samples at low magnification

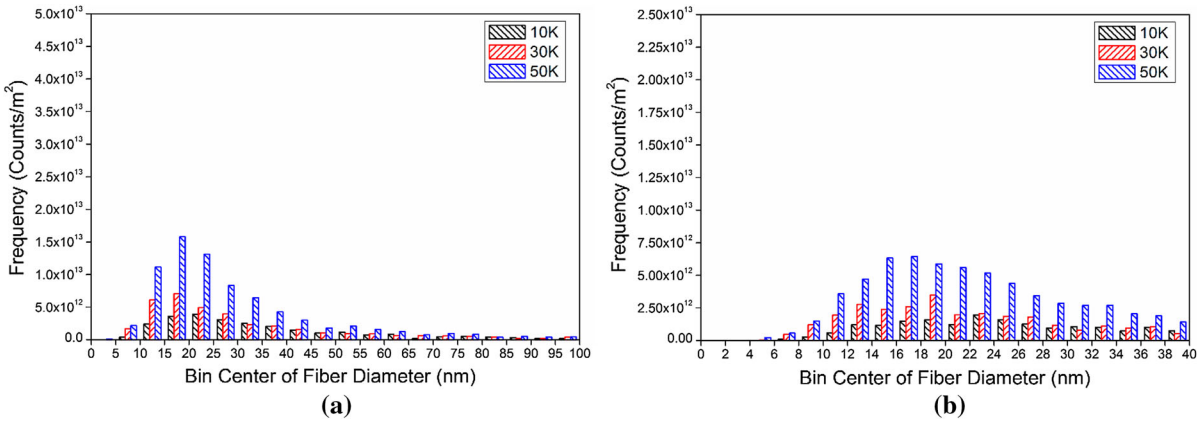

Fig. 5 Diameter distribution of refined BEK fibers based on high magnification SEM images sorted into **a** 5 nm and **b** 2 nm bin sizes

tendency and was used for all calculations as it is more robust in the presence of outliers. The choice of median is also supported by the histogram peak frequency bin center diameter values, which are shown to be much closer to the median as compared to the mean. These results are consistent with previous work done on NIST (National Institute of Standards and Technology) nanocellulose fibers produced using a valley beater (Zhang et al. 2012). Here, standard deviations were calculated to be larger than the arithmetic mean fiber diameter.

All high magnification fiber samples show a decrease in median fiber diameters with increasing mechanical energy consumption from refining and homogenization. From Table 3, the BEK 10K median nanocellulose fiber diameter of 31 nm reduces by 19% to 25 nm with BEK 30K, and by 45% to 17 nm with BEK 10K1P. With the larger fibers in Table 4, the BEK 10K median wood fiber diameter of 12,242 nm reduces by about 7.4% to 11,339 nm with BEK 30K and by about 80% to 2430 nm with BEK 10K1P. From Table 2, it can be seen that the increase in specific energy consumption from BEK 10K to BEK 30K (7083 kWh/t fiber) and BEK 10K to BEK 10K1P (7200 kWh/t fiber) was relatively equal. Hence, homogenization was shown to be more effective in

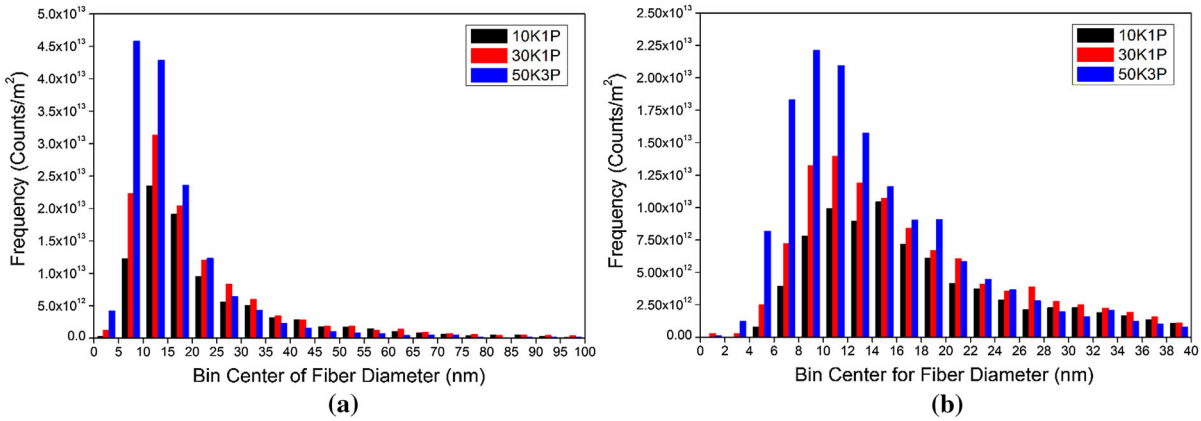

Fig. 6 Diameter distribution of refined and homogenized BEK fibers based on high magnification SEM images sorted into **a** 5 nm and **b** 2 nm bin sizes

reducing the median nanocellulose fiber diameters than PFI mill refining. As expected, the normalised fiber counts/m^2 increases with increasing energy consumption. Based on the smaller nanocellulose fibers in Table 3, the fiber counts/m^2 measured at 10^{13} with refining increases by approximately an order of magnitude to 10^{14} with homogenization. This shows that the homogenizer produces a greater proportion of smaller diameter nanocellulose fibers than the refiner, although both mechanical treatments reduce the fiber diameter with increasing energy consumption.

Sedimentation and gel point determination

The results of the sedimentation experiments are shown in Fig. 7. The first derivative of the curve at the y-intercept gives the gel point for each fiber sample. The aspect ratio (length/diameter) of each fiber sample was then calculated from the gel point, which allows for the estimation of indicative fiber length (Varanasi et al. 2013).

From Fig. 7, increasing the amount of mechanical refining and homogenization gradually reduces the gel point of the fibers, as evidenced by the decreasing slope of the trend lines. As expected, never-dried BEK 0K has the highest gel point (highest slope), and the most highly processed fiber BEK 50K3P has the lowest gel point (lowest slope). A lower gel point represents a higher aspect ratio. The BEK 10K, BEK 30K and BEK 50K samples had almost similar gel points. Homogenization however lowers the slope significantly for all three samples. A summary of the gel point values obtained is shown in Table 5.

From the literature, progressive refining and homogenization increases the surface charge of the fibrils (Dimic-Misic et al. 2018a). This results in an increase in fibril area and contact points available to entrap water (Dimic-Misic et al. 2016). The combination of immobilized water on the surface and water in the interfibril spacing produces gel-like behaviour within fibrillary matrices (Dimic-Misic et al. 2016). The gel point, also known as the connectivity threshold, is the lowest volume fraction where particles first form a continuous network (Varanasi et al. 2013). Gel point by sedimentation assumes gravity to be the dominant force (Raj et al. 2016). However, an increase in surface charge with progressive fibrillation results in a significant electrostatic repulsive force component (Raj et al. 2016). This causes the sediment height to increase for a given solids concentration across all samples. Again, while nanocellulose with high aspect ratios can be used for specific applications, certain rheological issues have been raised as a consequence of this increase in gel-like behaviour. Notably, an increase in suspension viscosity with progressive fiber fibrillation causes detrimental effects with press dewatering in papermaking at high sheet grammages (Rantanen and Maloney 2013). This further brings into question the necessity for such high aspect ratio and low diameter fibers to achieve high sheet strength due to these issues and the high energy cost of production.

Table 3 Summary of diameter distribution of unrefined, refined and homogenized BEK fibers based on 4 high magnification SEM images

BEK sample	High magnification (× 4 quadrant images)										
	Min diameter (nm)	Median diameter (nm)	Max diameter (nm)	Arithmetic mean diameter (nm)	Std error of mean (nm)	Std Dev (nm)	Skewness	Kurtosis	Total sample size (counts)	Normalized counts (m^2)	Histogram peak frequency bin center diameter (nm)
0K	9325	13,113	14,603	12,538.5	1189.88	2380	− 1.04	0.01	4	1.26×10^{11}	15,000
10K	7	31	1285	53.0	2.85	85	8.22	96.43	899	2.84×10^{13}	23
30K	6	25	672	43.5	1.75	62	5.76	44.55	1261	3.98×10^{13}	19
50K	4	24	622	33.6	0.77	38	7.38	84.01	2482	7.83×10^{13}	17
10K1P	4	17	392	25.8	0.49	27	4.57	34.12	2946	9.29×10^{13}	15
30K1P	3	16	313	23.1	0.37	23	4.54	34.42	3786	1.19×10^{14}	11
50K3P	2	12	298	16.6	0.22	15	5.78	60.11	4723	1.49×10^{14}	9

Table 4 Summary of diameter distribution of unrefined, refined and homogenized BEK fibers based on low magnification SEM image

BEK sample	Low magnification (×1 overview image)										
	Min diameter (nm)	Median diameter (nm)	Max diameter (nm)	Arithmetic mean diameter (nm)	Std error of mean (nm)	Std Dev (nm)	Skewness	Kurtosis	Total sample size (counts)	Normalized counts (m^2)	Histogram peak frequency bin center diameter (nm)
0K	9325	14,519	18,769	14,531	924	2924	− 0.22	− 0.408	10	1.07×10^7	15,000
10K	5970	12,242	17,731	12,086	872	3143	− 0.09	0.266	13	1.39×10^7	13,000
30K	7002	11,339	17,998	11,850	770	3080	0.38	− 0.398	16	1.71×10^7	11,000
50K	2302	8920	17,609	9381	1012	4410	0.47	− 0.304	19	2.03×10^7	9000
10K1P	1465	2430	16,164	5086	639	3834	1.77	2.443	20	2.14×10^7	3000
30K1P	1387	2924	5629	3085	180	1125	0.55	− 0.715	39	4.17×10^7	3000
50K3P	1231	2816	5386	2945	136	979	0.68	0.108	52	5.56×10^7	3000

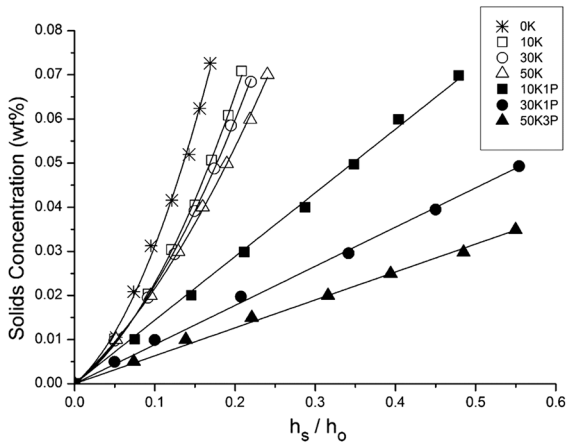

Fig. 7 Sedimentation behaviour of unrefined, refined and homogenized BEK fibers

Aspect ratio estimation

A summary of gel point, EMT average aspect ratio, median fiber diameter and indicative fiber length values is shown in Table 5. As shown in Table 5, the unrefined BEK 0K average aspect ratio of 84 increases by 21% to 102 with 10K refining but does not change significantly with further refining. Homogenization however greatly increases the aspect ratio of the fibers by 69% to 142 with BEK 10K1P, and by 173% to 229 with BEK 50K3P. From Table 2, it can be seen that the increase in specific energy consumption from BEK 10K to BEK 30K and BEK 10K to BEK 10K1P is approximately equal. Hence, homogenization was shown to be more effective in increasing fiber aspect ratio than PFI mill refining. Increasing the number of passes through a homogenizer can be used to produce nanocellulose fibers with high aspect ratios, indicating that fiber diameter reduction dominates over fiber shortening.

As previously mentioned, the indicative fiber lengths were estimated using the median fiber diameter and EMT fiber aspect ratio. It is worth noting that these estimations were performed merely to observe trends and should not be taken as absolute values. Estimations from the gel point measurements and high magnification SEM images show that all refined and homogenized fibers had approximately similar 2–3 μm fiber lengths. With the larger fibers in the low magnification SEM images, the indicative fiber lengths obtained with the homogenizer were notably shorter than those obtained from the refiner.

Sheet strength and mechanical properties

Figure 8 shows the representative stress–strain curve relationship for the average breaking load and strain at break for all fiber samples. Figures 9 and 10 shows the average tensile index and Young's modulus for unrefined, refined MFC and homogenized NFC fibers as function of density and specific energy consumption with 95% confidence intervals, respectively. It is worth noting that the Young's Modulus values shown in Figs. 9 and 10 were calculated as the average of multiple strips taken from 3 handsheets for each sample respectively. However, the representative curves shown in Fig. 8 were plotted using the stress–

Table 5 Gel point, aspect ratio and indicative fiber length estimation of BEK fiber samples

BEK fiber	Gel point, C_c (wt%)	EMT average aspect ratio, A	Median fiber diameter, d (nm)		Indicative fiber length, l [l = d × A] (μm)	
			High Mag.	Low Mag.	High Mag.	Low Mag.
0K	0.353	84	13,113	14,519	1101.5	1220
10K	0.256	102	31	12,242	3.2	1248
30K	0.243	105	25	11,339	2.6	1190
50K	0.230	108	24	8920	2.6	963
10K1P	0.144	142	17	2430	2.4	345
30K1P	0.089	188	16	2924	3.0	549
50K3P	0.063	229	12	2816	2.7	644

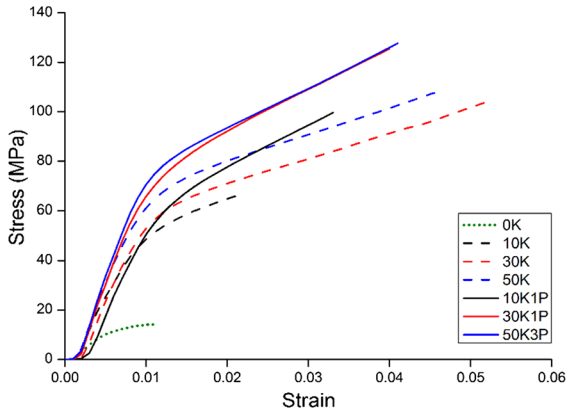

Fig. 8 Stress-strain curves for all BEK fiber samples

strain relationship of a strip which most closely follows that of the average value obtained for a particular sample. This was done for ease of trend identification between samples.

As shown in Fig. 8, the Young's modulus of the BEK fibers increases with progressive refining and homogenization. From Fig. 9a, all refined MFC sheets had an approximate threefold strength improvement, with an average tensile index of approximately 101 ± 8 Nm/g over conventional BEK 0K sheets. All homogenized NFC sheets had an approximate fourfold strength improvement with an average tensile index of approximately 119 ± 6 Nm/g over conventional BEK 0K sheets. In the case of the repeated BEK

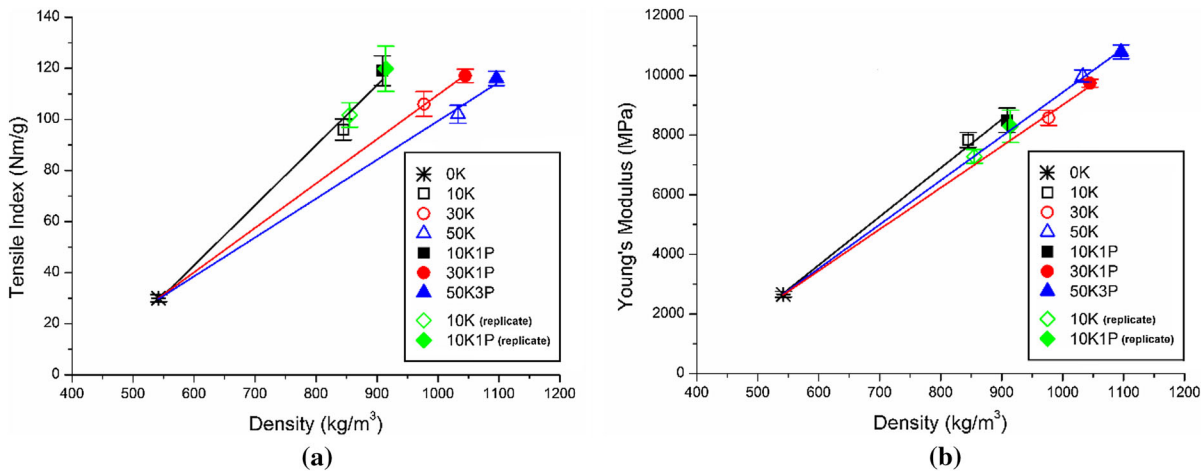

Fig. 9 Tensile index (**a**) and Young's modulus (**b**) as a function of density for all BEK fiber samples with 95% confidence interval error bars

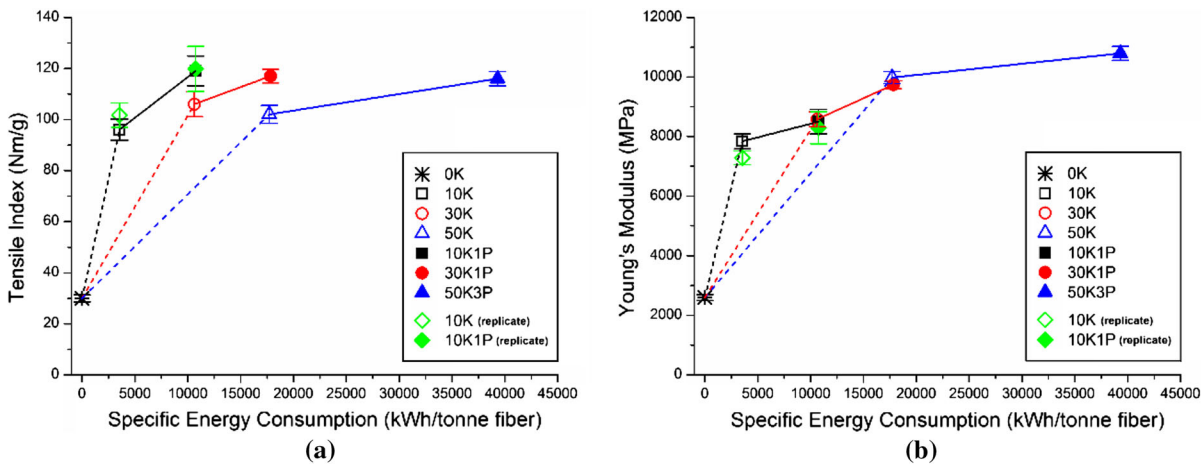

Fig. 10 Tensile index (**a**) and Young's modulus (**b**) as a function of specific energy consumption for all BEK fiber samples (*dotted line* effect of refining, *solid line* effect of homogenization) with 95% confidence interval error bars

10K and BEK 10K1P batches, the tensile index results were also consistent with that from the original batch at approximately 100 Nm/g and 120 Nm/g for BEK 10K and BEK 10K1P, respectively. These replicate values were also included as data points in Figs. 9 and 10.

Interestingly, BEK 10K1P with a lower sheet density compared to BEK 30K and BEK 50K, had a higher sheet tensile index. Correlating back to the energy consumption in Table 2, BEK 30K and BEK 10K1P had similar energy consumption values of approximately 10,000 kWh/t fiber despite BEK 30K sheets having a notably higher sheet density. As evidenced, refining is more effective in increasing sheet densification as compared to homogenization. This could be attributed to the progressive effects of fiber shortening with very heavy refining (Kerekes 2005) which increases fiber packing density. ANOVA analysis performed on the refined MFC (BEK 10K, BEK 30K, BEK 50K) versus the refined and homogenized NFC (BEK 10K1P, BEK 30K1P, BEK 50K3P) fiber tensile index data sets resulted in a p value of 5.38×10^{-15}, F value of 82.42 and F-critical value of 3.928. Here, the F value is significantly greater than the F-critical value, leading to a rejection of the null hypothesis. The results are shown to have a statistically significant difference between the refined MFC and the refined and homogenized NFC fiber samples.

From Fig. 9b, the Young's modulus was shown to increase with sheet densification from both refining and homogenization. For a fixed sheet grammage of 60 gsm, an increase in density reduces the cross-sectional area which improves the strength, even if the breaking load has not changed. Also, a denser network would promote the formation of more fiber–fiber bonds which has been well established to increase the Young's modulus of the cellulose fiber material (Niskanen 1998). This is due to an efficiency improvement in dissipating and transferring stresses uniformly throughout the fiber network.

When correlating specific energy consumption to the increase in tensile index of handsheets in Fig. 10a, surprisingly BEK 50K3P sheets had only relatively marginal improvements of approximately 20% over BEK 10K sheets but required a more than tenfold increase in mechanical energy consumption to make. This is despite the fiber aspect ratio, which is believed to control the efficiency of stress transfer in the network, increasing significantly by 124% from 102 to 229. Further, a more than twofold decrease in median nanocellulose fiber diameters from 31 to 12 nm was observed, which would result in significantly larger fiber surface area available for bonding. However, there is little to no evidence to suggest that sheet strength behaves in accordance with the pronounced developments in nanocellulose fiber quality, as had been initially expected.

Consequently, a constant increase in mechanical energy consumption with refining and homogenization does not correlate to a progressive increase in mechanical properties. This is despite the progressively smaller nanocellulose fiber diameters and higher fiber aspect ratio. These results confirm that the PFI mill refiner is more effective than the homogenizer in producing nanocellulose for high strength applications, measured and compared from a specific energy consumption and sheet tensile index perspective. Future work might be to investigate the effect of different pulp sources (such as chemical, thermomechanical, bleached, unbleached, hardwoods and softwoods) and hemicellulose content (Klemm et al. 2011; Lavoine et al. 2012) on the strength properties and fibrillation degree.

Conclusion

Bleached eucalyptus Kraft (BEK) pulp samples were refined at a range of 10,000 to 50,000 revolutions and passed through a high pressure homogenizer between 1 and 3 passes. Results from thorough SEM image analysis of over 16,000 fibers showed that the initial unrefined median fiber diameter of 13,113 nm decreased significantly to 31 nm (in the case of the least heavily refined fibers) and 12 nm (in the case of the most heavily refined and homogenized fibers). The least heavily refined fibers' aspect ratio was shown to increase by 21%, and the most heavily refined and homogenized fibers' aspect ratio increased by 173% over the unrefined wood fibers with sedimentation experiments. The Young's modulus of all fiber sheets increased with increasing densification. Interestingly, all refined samples had a tensile index of around 100 Nm/g, a more than threefold increase over unrefined wood fiber sheets. All additional homogenization treatment further increased this value by only 20% despite the significant developments fiber quality. This was surprising considering the most heavily treated

fibers (50,000 PFI revolutions and 3 homogenization passes at 1000 bar) required a more than tenfold increase in energy consumption to produce over the least heavily treated fibers (10,000 PFI revolutions).

Here most importantly, we have shown that nanocellulose sheet strength does not behave in accordance with the developments in fiber quality with increasing energy consumption. This is evidenced by the approximately constant tensile index values of all refined sheets despite the observed changes in fiber fibrillation with progressive refining. This study confirms that while an increase in specific energy consumption from homogenization can be used to tailor nanocellulose fibers with progressively smaller diameters and high aspect ratios for certain applications, very strong nanocellulose sheets can be produced from heavily refined fibers with significantly lower energy.

We believe this work sheds light and counteracts the common misconception that very high energy consumption is necessary for good nanocellulose sheet strength. Interestingly, this work has the potential to reinvigorate further interest and research into refining, a mature and well established technology in the pulp and paper industry. While the production of nanocellulose is still not without its challenges, it is crucial that the energy cost to performance criteria for nanocellulose be properly addressed in order to compete with the economies of scale of existing fossil-fuel based materials. Here we have shown that these cellulose materials of the future can be produced at lower energy while still retaining all its remarkable strength properties in hopes of not only achieving environmentally friendly but economically sustainable production.

Acknowledgments The authors wish to thank Australian Paper Maryvale for their support and funding for the research project. The authors also wish to acknowledge the Monash Centre of Electron Microscopy (MCEM) for use of their SEM facilities. Shaun Ang would like to thank the Australian Government for a Research Training Program (RTP) scholarship.

References

Alemdar A, Sain M (2008) Isolation and characterization of nanofibers from agricultural residues—wheat straw and soy hulls. Biores Technol 99:1664–1671. https://doi.org/10.1016/j.biortech.2007.04.029

Andresen M, Stenius P (2007) Water-in-oil emulsions stabilized by hydrophobized microfibrillated cellulose. J Dispers Sci Technol 28:837–844. https://doi.org/10.1080/01932690701341827

Ankerfors M (2012) Microfibrillated cellulose energy-efficient preparation techniques and key properties. KTH Royal Institute of Technology, Stockholm

Aulin C, Gällstedt M, Lindström T (2010) Oxygen and oil barrier properties of microfibrillated cellulose films and coatings. Cellulose 17:559–574. https://doi.org/10.1007/s10570-009-9393-y

Campano C et al (2018) Mechanical and chemical dispersion of nanocelluloses to improve their reinforcing effect on recycled paper. Cellulose 25:269–280. https://doi.org/10.1007/s10570-017-1552-y

Celzard A, Fierro V, Kerekes R (2009) Flocculation of cellulose fibres: new comparison of crowding factor with percolation and effective-medium theories. Cellulose 16:983–987. https://doi.org/10.1007/s10570-009-9314-0

Chang CP, Wang IC, Perng YS (2013) Enhanced thermal behavior, mechanical properties and UV shielding of polylactic acid (PLA) Composites reinforced with nanocrystalline cellulose and filled with nanosericite. Cellul Chem Technol 47:111–123

Dimic-Misic K, Gane PAC, Paltakari J (2013) Micro and nanofibrillated cellulose as a rheology modifier additive in CMC-containing pigment-coating formulations. Ind Eng Chem Res 52:16066–16083. https://doi.org/10.1021/ie4028878

Dimic-Misic K, Ridgway C, Maloney T, Paltakari J, Gane P (2014) Influence on pore structure of micro/nanofibrillar cellulose in pigmented coating formulations. Transp Porous Media 103:155–179. https://doi.org/10.1007/s11242-014-0293-8

Dimic-Misic K, Rantanen J, Maloney TC, Gane PAC (2016) Gel structure phase behavior in micro nanofibrillated cellulose containing in situ precipitated calcium carbonate. J Appl Polym Sci. https://doi.org/10.1002/app.43486

Dimic-Misic K, Maloney T, Gane P (2018a) Effect of fibril length, aspect ratio and surface charge on ultralow shear-induced structuring in micro and nanofibrillated cellulose aqueous suspensions. Cellulose 25:117–136. https://doi.org/10.1007/s10570-017-1584-3

Dimic-Misic K, Vanhatalo K, Dahl O, Gane P (2018b) Rheological properties comparison of aqueous dispersed nanocellulose derived from a novel pathway-produced microcrystalline cellulose or by conventional methods. Appl Rheol. https://doi.org/10.3933/applrheol-28-64474

Eichhorn SJ et al (2001) Current international research into cellulosic fibres and composites. J Mater Sci 36:2107–2131. https://doi.org/10.1023/A:1017512029696

Eichhorn SJ et al (2010) Review: Current international research into cellulose nanofibres and nanocomposites. J Mater Sci 45:1–33. https://doi.org/10.1007/s10853-009-3874-0

El Baradai O, Beneventi D, Alloin F, Bongiovanni R, Bruas-Reverdy N, Bultel Y, Chaussy D (2016) Microfibrillated cellulose based ink for eco-sustainable screen printed flexible electrodes in lithium ion batteries. J Mater Sci Technol 32:566–572. https://doi.org/10.1016/j.jmst.2016.02.010

Eriksen Ø, Syverud K, Gregersen Ø (2008) The use of microfibrillated cellulose produced from kraft pulp as strength enhancer in TMP paper. Nord Pulp Pap Res J 23:299–304

Ferrer A, Filpponen I, Rodríguez A, Laine J, Rojas OJ (2012) Valorization of residual empty palm fruit bunch fibers (EPFBF) by microfluidization: production of nanofibrillated cellulose and EPFBF nanopaper. Bioresour Technol 125:249–255. https://doi.org/10.1016/j.biortech.2012.08.108

Henriksson M, Henriksson G, Berglund LA, Lindström T (2007) An environmentally friendly method for enzyme-assisted preparation of microfibrillated cellulose (MFC) nanofibers. Eur Polym J 43:3434–3441. https://doi.org/10.1016/j.eurpolymj.2007.05.038

Henriksson M, Berglund LA, Isaksson P, Lindström T, Nishino T (2008) Cellulose nanopaper structures of high toughness. Biomacromolecules 9:1579–1585. https://doi.org/10.1021/bm800038n

Hubbe MA, Tayeb P, Joyce M, Tyagi P, Kehoe M, Dimic-Misic K, Pal L (2017) Rheology of nanocellulose-rich aqueous suspensions: a review. BioResources 12:9556–9661. https://doi.org/10.15376/biores.12.4.Hubbe

Isogai A, Saito T, Fukuzumi H (2011a) TEMPO-oxidized cellulose nanofibers. Nanoscale 3:71–85. https://doi.org/10.1039/c0nr00583e

Isogai T, Saito T, Isogai A (2011b) Wood cellulose nanofibrils prepared by TEMPO electro-mediated oxidation. Cellulose 18:421–431. https://doi.org/10.1007/s10570-010-9484-9

Iwamoto S, Nakagaito AN, Yano H, Nogi M (2005) Optically transparent composites reinforced with plant fiber-based nanofibers. Appl Phys A Mater Sci Process 81:1109–1112. https://doi.org/10.1007/s00339-005-3316-z

Iwamoto S, Nakagaito AN, Yano H (2007) Nano-fibrillation of pulp fibers for the processing of transparent nanocomposites. Appl Phys A Mater Sci Process 89:461–466. https://doi.org/10.1007/s00339-007-4175-6

Iwamoto S, Abe K, Yano H (2008) The effect of hemicelluloses on wood pulp nanofibrillation and nanofiber network characteristics. Biomacromol 9:1022–1026. https://doi.org/10.1021/bm701157n

Karande VS, Bharimalla AK, Hadge GB, Mhaske ST, Vigneshwaran N (2011) Nanofibrillation of cotton fibers by disc refiner and its characterization. Fibers Polym 12:399–404. https://doi.org/10.1007/s12221-011-0399-3

Karande VS, Mhaske ST, Bharimalla AK, Hadge GB, Vigneshwaran N (2013) Evaluation of two-stage process (refining and homogenization) for nanofibrillation of cotton fibers. Polym Eng Sci 53:1590–1597. https://doi.org/10.1002/pen.23413

Kerekes RJ (2005) Characterizing refining action in PFI mills. Tappi J 4:9–14

Kerekes RJ (2015) Perspectives on high and low consistency refining in mechanical pulping. BioResources. https://doi.org/10.15376/biores.10.4.8795-8811

Klemm D, Kramer F, Moritz S, Lindström T, Ankerfors M, Gray D, Dorris A (2011) Nanocelluloses: a new family of nature-based materials. Angew Chem Int Ed 50:5438–5466. https://doi.org/10.1002/anie.201001273

Kumar V et al (2014) Comparison of nano- and microfibrillated cellulose films. Cellulose 21:3443–3456. https://doi.org/10.1007/s10570-014-0357-5

Lavoine N, Desloges I, Dufresne A, Bras J (2012) Microfibrillated cellulose—its barrier properties and applications in cellulosic materials: a review. Carbohyd Polym 90:735–764. https://doi.org/10.1016/j.carbpol.2012.05.026

Lee SY, Chun SJ, Kang IA, Park JY (2009) Preparation of cellulose nanofibrils by high-pressure homogenizer and cellulose-based composite films. J Ind Eng Chem 15:50–55. https://doi.org/10.1016/j.jiec.2008.07.008

Lewis L, Derakhshandeh M, Hatzikiriakos SG, Hamad WY, MacLachlan MJ (2016) Hydrothermal gelation of aqueous cellulose nanocrystal suspensions. Biomacromolecules 17:2747–2754. https://doi.org/10.1021/acs.biomac.6b00906

Lindström T (2017) Aspects on nanofibrillated cellulose (NFC) processing, rheology and NFC-film properties. Curr Opin Colloid Interface Sci 29:68–75. https://doi.org/10.1016/j.cocis.2017.02.005

Martinez D et al (2001) Characterizing the mobility of papermaking fibres during sedimentation. In: The science of papermaking: transactions of the 12th fundamental research symposium, Oxford. The Pulp and Paper Fundamental Research Society, Bury, UK, pp 225–254

Nakagaito AN, Yano H (2005) Novel high-strength biocomposites based on microfibrillated cellulose having nano-order-unit web-like network structure. Appl Phys A Mater Sci Process 80:155–159. https://doi.org/10.1007/s00339-003-2225-2

Nelson K, Retsina T, Iakovlev M, van Heiningen A, Deng Y, Shatkin JA, Mulyadi A (2016) American process: production of low cost nanocellulose for renewable, advanced materials applications. In: Madsen L, Svedberg E (eds) Materials research for manufacturing. Springer series in materials science, vol 224. Springer, Cham. https://doi.org/10.1007/978-3-319-23419-9_9

Niskanen K (1998) Papermaking science and technology, paper physics vol 16. Forest Products Engineers Finland, Helsinki

Nogi M, Iwamoto S, Nakagaito AN, Yano H (2009) Optically transparent nanofiber paper. Adv Mater 21:1595–1598. https://doi.org/10.1002/adma.200803174

Osong SH, Norgren S, Engstrand P (2016) Processing of wood-based microfibrillated cellulose and nanofibrillated cellulose, and applications relating to papermaking: a review. Cellulose 23:93–123. https://doi.org/10.1007/s10570-015-0798-5

Pääkko M et al (2007) Enzymatic hydrolysis combined with mechanical shearing and high-pressure homogenization for nanoscale cellulose fibrils and strong gels. Biomacromolecules 8:1934–1941. https://doi.org/10.1021/bm061215p

Page DH (1969) A theory for the tensile strength of paper. Tappi J 52:674–681

Raj P, Varanasi S, Batchelor W, Garnier G (2015) Effect of cationic polyacrylamide on the processing and properties of nanocellulose films. J Colloid Interface Sci 447:113–119. https://doi.org/10.1016/j.jcis.2015.01.019

Raj P, Mayahi A, Lahtinen P, Varanasi S, Garnier G, Martin D, Batchelor W (2016) Gel point as a measure of cellulose nanofibre quality and feedstock development with mechanical energy. Cellulose 23:3051–3064. https://doi.org/10.1007/s10570-016-1039-2

Ramires EC, Dufresne A (2011) A review of cellulose nanocrystals and nanocomposites. Tappi J 10:9–16

Rantanen J, Maloney TC (2013) Press dewatering and nip rewetting of paper containing nano- and microfibril cellulose. Nord Pulp Pap Res J 28:582–587

Rantanen J, Dimic-Misic K, Pirttiniemi J, Kuosmanen P, Maloney TC (2015) Forming and dewatering of a microfibrillated cellulose composite paper. BioResources 10:3492–3506. https://doi.org/10.15376/biores.10.2.3492-3506

Shanmugam K, Doosthosseini H, Varanasi S, Garnier G, Batchelor W (2018) Flexible spray coating process for smooth nanocellulose film production. Cellulose 25:1725–1741. https://doi.org/10.1007/s10570-018-1677-7

Siqueira G, Bras J, Dufresne A (2009) Cellulose whiskers versus microfibrils: influence of the nature of the nanoparticle and its surface functionalization on the thermal and mechanical properties of nanocomposites. Biomacromolecules 10:425–432. https://doi.org/10.1021/bm801193d

Siró I, Plackett D (2010) Microfibrillated cellulose and new nanocomposite materials: a review. Cellulose 17:459–494. https://doi.org/10.1007/s10570-010-9405-y

Siró I, Plackett D, Hedenqvist M, Ankerfors M, Lindström T (2011) Highly transparent films from carboxymethylated microfibrillated cellulose: the effect of multiple homogenization steps on key properties. J Appl Polym Sci 119:2652–2660. https://doi.org/10.1002/app.32831

Spence KL, Venditti RA, Habibi Y, Rojas OJ, Pawlak JJ (2010) The effect of chemical composition on microfibrillar cellulose films from wood pulps: mechanical processing and physical properties. Biores Technol 101:5961–5968. https://doi.org/10.1016/j.biortech.2010.02.104

Spence KL, Venditti RA, Rojas OJ, Habibi Y, Pawlak JJ (2011) A comparative study of energy consumption and physical properties of microfibrillated cellulose produced by different processing methods. Cellulose 18:1097–1111. https://doi.org/10.1007/s10570-011-9533-z

Stelte W, Sanadi AR (2009) Preparation and characterization of cellulose nanofibers from two commercial hardwood and softwood pulps. Ind Eng Chem Res 48:11211–11219. https://doi.org/10.1021/ie9011672

Su J, Mosse WKJ, Sharman S, Batchelor WJ, Garnier G (2013) Effect of tethered and free microfibrillated cellulose (MFC) on the properties of paper composites. Cellulose 20:1925–1935. https://doi.org/10.1007/s10570-013-9955-x

Syverud K, Stenius P (2009) Strength and barrier properties of MFC films. Cellulose 16:75–85. https://doi.org/10.1007/s10570-008-9244-2

Syverud K, Chinga-Carrasco G, Toledo J, Toledo PG (2011) A comparative study of Eucalyptus and Pinus radiata pulp fibres as raw materials for production of cellulose nanofibrils. Carbohyd Polym 84:1033–1038. https://doi.org/10.1016/j.carbpol.2010.12.066

Taipale T, Österberg M, Nykänen A, Ruokolainen J, Laine J (2010) Effect of microfibrillated cellulose and fines on the drainage of kraft pulp suspension and paper strength. Cellulose 17:1005–1020. https://doi.org/10.1007/s10570-010-9431-9

TAPPI (2001a) T 248 sp-00 Laboratory Beating of Pulp (PFI Mill Method). Technical Association of the Pulp and Paper Industry (TAPPI) Press, Technology Park, Atlanta, GA, USA

TAPPI (2001b) T 402 sp-98 Standard conditioning and testing atmospheres for paper, board, pulp handsheets, and related products. Technical Association of the Pulp and Paper Industry (TAPPI) Press, Technology Park, Atlanta, GA, USA

TAPPI (2001c) T 494 om-96 Tensile Breaking Properties of Paper and Paperboard (Using Constant Rate of Elongation Apparatus). Technical Association of the Pulp and Paper Industry (TAPPI) Press, Technology Park, Atlanta, GA, USA

Varanasi S, He R, Batchelor W (2013) Estimation of cellulose nanofibre aspect ratio from measurements of fibre suspension gel point. Cellulose 20:1885–1896. https://doi.org/10.1007/s10570-013-9972-9

Varanasi S, Henzel L, Sharman S, Batchelor W, Garnier G (2018) Producing nanofibres from carrots with a chemical-free process. Carbohyd Polym 184:307–314. https://doi.org/10.1016/j.carbpol.2017.12.056

Vartiainen J, Lahtinen P, Kaljunen T, Kunnari V, Peresin MS, Tammelin T (2015) Comparison of properties between cellulose nanofibrils made from banana, sugar beet, hemp, softwood and hardwood pulps. O Pap 76:57–60

Vigneshwaran N, Satyamurthy P, Jain P (2015) Biological synthesis of nanocrystalline cellulose by controlled hydrolysis of cotton fibers and linters. In: Handbook of polymer nanocomposites. Processing, performance and application: volume C: polymer nanocomposites of cellulose nanoparticles, pp 27–36. https://doi.org/10.1007/978-3-642-45232-1_62

Walker C (2012) Thinking small is leading to big changes. Paper 360(7):8–13

Zhang L, Batchelor W, Varanasi S, Tsuzuki T, Wang X (2012) Effect of cellulose nanofiber dimensions on sheet forming through filtration. Cellulose 19:561–574. https://doi.org/10.1007/s10570-011-9641-9